Disabled-2 small interfering RNA modulates cellular adhesive function and MAPK activity during megakaryocytic differentiation of K562 cells

Ching-Ping Tseng[a,b,*], Chien-Ling Huang[a], Ching-Hui Huang[b], Ju-Chien Cheng[c], Arnold Stern[d], Chin-Hsiao Tseng[e], Daniel Tsun-Yee Chiu[a]

[a] *Graduate Institute of Medical Biotechnology Chang Gung University, 259 Wen-Hwa 1st Road, Kweishan, Taoyuan 333, Taiwan*
[b] *Graduate Institute of Basic Medical Sciences, Chang Gung University, Taoyuan, Taiwan*
[c] *Department of Medical Technology, China Medical College, Taichung, Taiwan*
[d] *Department of Pharmacology, New York University School of Medicine, New York, NY, USA*
[e] *Department of Internal Medicine, National Taiwan University, Taipei, Taiwan*

Received 17 January 2003; revised 10 March 2003; accepted 12 March 2003

First published online 24 March 2003

Edited by Veli-Pekka Lehto

Abstract Previous studies have shown that Disabled-2 (DAB2) is up-regulated during megakaryocytic differentiation of human K562 cells. To delineate the consequences of DAB2 induction, a DNA vector-based small interfering RNA (siRNA) was designed to intervene in DAB2 expression. We found that DAB2 siRNA specifically inhibited DAB2 induction, resulting in the modulation of cell–cell adhesion and mitogen-activated protein kinase (MAPK) phosphorylation. The morphological changes and β3 integrin expression associated with megakaryocytic differentiation were not affected. Since the MAPK pathway has been shown to involve DAB2 induction [Tseng et al., Biochem. Biophys. Res. Commun. 285 (2001) 129–135], our results suggest a reciprocal regulation between DAB2 and MAPK in the differentiation of K562 cells. In addition, we have demonstrated for the first time that DAB2 siRNA is a valuable tool for unveiling the biological consequences of DAB2 expression.

Key words: Disabled-2; Small interfering RNA; K562 cell; Megakaryocytic differentiation; Mitogen-activated protein kinase

1. Introduction

Disabled-2 (DAB2) is a cytoplasmic adapter protein mediating epidermal growth factor, colony stimulating factor-1, and transforming growth factor-β cellular signals [1–4]. Like other adapter proteins, DAB2 has no catalytic activity but elicits its function through interaction and modulation of other cellular proteins. Mediated by the N-terminal phosphotyrosine interacting domain, DAB2 interacts with the RAS GTPase-activating protein DIP1/2 as well as the SMAD family of transcription factors. These interactions have significant functional impact on gene transcription [3,5]. Through the C-terminus proline-rich sequences, DAB2 interacts with myosin VI and the adapter protein GRB2 resulting in the modulation of cellular activity [6–8]. The function of DAB2 is also regulated by both the p42/p44 mitogen-activated protein kinase (MAPK) pathway and protein kinase C-mediated protein phosphorylation [8,9]. For instance, phosphorylation of DAB2 at serine 24 in the N-terminus of DAB2 was shown to be the key amino acid residue in modulating AP-1 transcriptional activity [8]. These studies suggest that DAB2 involves multiple signaling pathways and modulates cellular functions through several distinct mechanisms.

The level of DAB2 has significant impact on cancer development and hematopoietic cell differentiation. Aberration of DAB2 expression has been shown to associate with breast, prostate, and mouse mammary tumors. Expression of DAB2 in cancer cell lines resulted in cell cycle arrest and a decreased rate of cell growth [10,11]. On the other hand, during megakaryocytic differentiation of the human chronic myeloid leukemic cell line K562, DAB2 is up-regulated in a p42/p44 MAPK-dependent manner [9]. The significance of DAB2 induction in hematopoietic cell differentiation and signaling has not yet been addressed. This is partly due to the lack of simple and valuable genetic tools to disrupt DAB2 expression for analyzing cellular function.

Recent studies have revealed that RNA interference (RNAi), a process of homology-dependent degradation of cognate mRNA by double-stranded RNA (dsRNA), is a powerful tool in the down-regulation of gene expression [12]. This phenomenon is commonly present in nematodes, plants and fungi. In mammalian cells, it was recently shown that introduction of a small interfering RNA (siRNA), generally 21–23 nt, could achieve a similar gene inhibitory effect without the non-specific activation of dsRNA-activated protein kinase R [13]. In this study, a DNA vector-based DAB2 siRNA is designed and generated for the first time that specifically inhibits DAB2 expression. Utilizing the DAB2 siRNA, we demonstrate a role of DAB2 in the control of cellular adhesive function. The present study also reveals a reciprocal regulation between DAB2 and MAPK during megakaryocytic differentiation of K562 cells.

2. Materials and methods

2.1. Materials

K562, HL-60, and MEG-01 cells were from the American Type Culture Collection (Manassas, VA, USA). HEL cells were a kind gift from Dr. H. Wu (Department of Pharmacy, Chia Nan University of Pharmacy and Science, Tainan, Taiwan). p42/p44 MAPK and phospho-p42/p44 MAPK antibodies were from New England BioLabs (Beverly, MA, USA). The DAB2 antibody p96 was from Trans-

*Corresponding author. Fax: (886)-3-2118355.
E-mail address: ctseng@mail.cgu.edu.tw (C.-P. Tseng).

0014-5793/03/$22.00
doi:10.1016/S0014-5793(03)00281-3

duction Laboratories (Lexington, KY, USA). The β3 antibody was from Santa Cruz Biotechnologies (Santa Cruz, CA, USA). 12-*O*-Tetradecanoylphorbol 13-acetate (TPA) and other molecular biology grade chemicals were from Sigma (St. Louis, MO, USA). The scramblase expression plasmid pCI-neo-His9 has been described previously [14]. pEGFP-C3 and pDsRed1-N1 were from Clontech (Palo Alto, CA, USA). The DMRIE-C and Lipofectamine 2000 (LF2000) transfection reagents were from Invitrogen (Carlsbad, CA, USA). FITC-labeled phosphorothioate oligonucleotides (S-oligos) were from Genasia (Taipei, Taiwan). Peptide nucleic acids (PNA) were from Applied Biosystems (Foster City, CA, USA).

2.2. Plasmid construction

For pCI-neo-hDAB2, human DAB2 cDNA was amplified by polymerase chain reaction (PCR) and then subcloned into the *Xho*I site of pCI-neo (Promega). For pTOPO-U6, the RNAi expression cassette containing the mouse U6 promoter and the termination signal of RNA polymerase III was inserted into the pCRII-TOPO vector (Invitrogen) with the following procedures. First, the mouse U6 promoter (−315 to +1) was PCR-amplified with the primer set U6-sense (5′-AGATCTATCCGACGCCGCCATCTCTA-3′) and U6-antisense (5′-GGATTGGTCTTCGATATCCAAACAAGGCTTTTCTCCAA-3′) using genomic DNA from mouse 3T3-L1 cells as the template. The PCR product was subcloned into the pCRII-TOPO vector by the TOPO cloning technique. Due to the enclosure of the recognition sequences for *Bbs*I and *Eco*RV in the U6-antisense PCR primer, these sites were created at the 3′-end of the promoter and the 5′-end of the *Not*I recognition sequence located at the multiple cloning sites. For inserting the -TTTTT termination sequences of RNA polymerase III, we annealed the complementary oligonucleotides TS (5′-ATCC-TTTTTTCACGTAGTGGC-3′) and TAS (5′-GGCCGCCACTACG-TGAAAAAA-3′). The annealing reaction generated TS/TAS dsDNA with overhang sequences for *Bbs*I and *Not*I sites that was ready for ligating to the *Bbs*I- and *Not*I-digested pCRII-TOPO plasmid with the U6 promoter. These steps resulted in the RNAi expression vector pTOPO-U6 that had the *Eco*RV and *Bbs*I sites for insertion of RNAi sequences. In addition, *Bgl*II and *Dra*III cloning sites were designed for release of the complete RNAi expression cassette and for the insertion into other expression vectors. For the plasmids Dab2–419 and Dab2–2112, the complementary oligonucleotides Dab2–419S (5′-CTGGGTAACATTTCCCTCAAGCTTCAGGGAA-ATGTTGACCCAG-3′) and Dab2–419AS (5′-GGATCTGGGTA-ACATTTCCCTGAAGCTTGAGGGAAATGTTGACCCAG-3′), as well as Dab2–2112S (5′-TTCCAACTGCGGCAGCCACAAGCTT-CTGGCTGCCGCAGTTGGAA-3′) and Dab2–2112AS (5′-GGA-TTTCCAACTGCGGCAGCCAGAAGCTTGTGGCTGCCGCAGT-TGGA-A-3′) were annealed, respectively. The annealing of Dab2–2112S/Dab2–2112AS or Dab2–419S/Dab2–419AS generated sites corresponding to the blunt end and the overhang that matched the *Eco*RV- and *Bbs*I-digested pTOPO-U6. The ligation between the annealed oligonucleotides and pTOPO-U6 at the *Eco*RV and *Bbs*I cloning sites generated Dab2–2112 and Dab2–419, respectively. For pEGFPC3-DAB2, the human DAB2 cDNA from pCI-neo-hDAB2 was inserted into the *Xho*I-*Bam*HI site of pEGFP-C3.

2.3. S-oligos and PNA transfection

For transfection of S-oligos, K562 cells were incubated with 4 μM FITC-labeled S-hDAB2 (5′-AsTGsTCsTAsACsGAsAGsTAsGA-sAAsC-3′) or AS-hDAB2 (5′-GsTTsTCsTAsCTsTCsGTsTAsGAs-CAsT-3′) in the presence of DMRIE-C for 7 h. The uptake efficiency of the S-oligos was monitored by fluorescence microscopy. For PNA transfection, K562 cells were transfected with 10 μM PNA1 (5′-CTACTTCGTTAGACATG-Lys-Lys-Lys-3′) and 10 μM PNA2 (5′-AGCATGACTTCCCCGC-Lys-Lys-Lys-3′) in the presence of LF2000 for 24 h. Cells were harvested for Western blot analysis after indicated treatments.

2.4. Transient transfection, preparation of cell extracts, and Western blot analysis

K562 and its subline D-1-4 that barely expressed DAB2 (C.H. Lee and C.P. Tseng, unpublished data) were cultured as described previously [9]. For transfection, K562 cells were plated at a density of 2×10^6/35 mm plate and were applied with 6 μg DNA premixed with 10 μl LF2000. Twenty-four hours later, the transfected cells were split and cultured at a density of 1.5×10^4/ml followed by the indicated treatments. The preparation of cell extracts and Western blot analysis were performed as described previously [9].

2.5. Cell aggregation and cell adhesion assay

The transfected cells were adjusted to a density of 3×10^4/ml. Following the indicated treatment for 24 and 48 h, cell clusters with >5 cells/aggregate were counted under phase contrast microscopy at a $40\times$ magnification power. For quantification of cell aggregation, the total numbers of cell clusters in 10 randomly selected fields were determined. For quantification of cell adhesion, the cells spreading on the culture dish were counted under phase contrast microscopy at a $100\times$ magnification power. The total numbers of spreading cells in 10 randomly selected fields were used as the index for cell adhesion.

3. Results

3.1. Design and characterization of DAB2 siRNA

The RNAi technique was recently adapted for modulation of gene expression in mammalian cells. We generated the DNA vector-based siRNAs Dab2–419 and Dab2–2112 and evaluated whether they are the effective DAB2 modulators (Fig. 1A,B). Sequence analysis revealed that Dab2–419 has a point deletion that resulted in a mismatch in the dsRNA region. To determine the inhibitory effect and specificity of DAB2 siRNAs, either Dab2–419 or Dab2–2112 was co-transfected with DAB2 and T7-Tag scramblase expression plasmids into D-1-4 cells with a ratio of 5:1:1, 10:1:1 and 25:1:1, respectively. Western blot analysis revealed that Dab2–2112 but not Dab2–419 inhibited DAB2 expression (Fig. 1C). Besides, both Dab2–419 and Dab2–2112 had no effect on the expression of T7-Tag scramblase of which the mRNA does not contain the target sequences of Dab2 siRNA.

The specificity of Dab2–2112 was further evaluated using the enhanced green fluorescent protein (EGFP) expression system. In our preliminary study, we found that Dab2–2112 did not inhibit EGFP expression (data not shown). We thus determined whether the fusion of DAB2 cDNA to the EGFP coding sequences switches EGFP to become a target of Dab2–2112. The pEGFPC3-DAB2 encoding EGFP-DAB2 fusion protein was co-transfected with pDsRed1-N1 into K562 cells in the presence of Dab2–2112 (Fig. 1D). The fluorescent intensity was observed with fluorescence microscopy 48 h after transfection. We found that the red fluorescent protein (RFP) encoded by pDsRed1-N1 is expressed at a comparable level in cells transfected with Dab2–2112 and vector control, indicating a similar efficiency of the transfections. The results also suggest that Dab2–2112 did not interfere with RFP expression. On the other hand, the fluorescent intensity of EGFP-DAB2 was significantly reduced in cells expressing Dab2–2112. Therefore, our results suggest that Dab2–2112 specifically modulates DAB2 expression.

3.2. DAB2 siRNA inhibits TPA-induced DAB2 expression in myeloid leukemic cells

Since DAB2 is expressed at various levels in different cell types, the expression patterns of DAB2 in several myeloid leukemic cells, including K562, MEG-01, HL-60, and HEL cells, were determined (Fig. 2A). At the exponential growth phase, K562 and MEG-01 cells had a low level of DAB2, while HEL cells showed intermediate DAB2 expression. HL-60 cells had no detectable DAB2. Upon TPA-mediated megakaryocytic differentiation of K562, MEG-01, and HEL cells, DAB2 induction was associated with the differentiation pro-

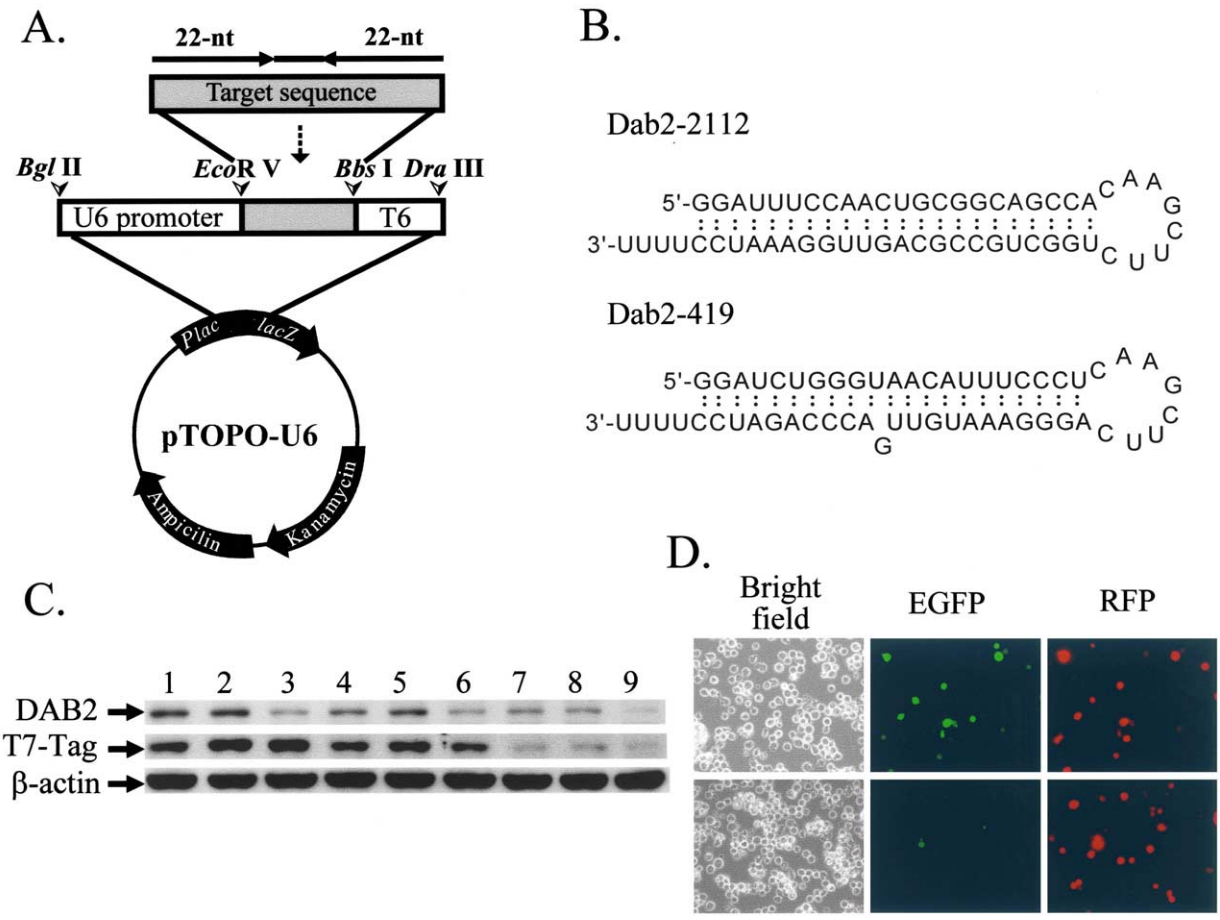

Fig. 1. Design and characterization of DAB2 siRNA. A: Schematic representation of DAB2 siRNA expression plasmid. The plasmid was designed and constructed as described in Section 2. B: Proposed DAB2 siRNA structures. The putative structures of the dsRNAs formed by Dab2–2112 and Dab2–419 were shown. C: Specific inhibition of DAB2 expression by DAB2 siRNA. D-1-4 cells were transfected for 48 h with pTOPO-U6 (lanes 1, 4, 7), Dab2–419 (lanes 2, 5, 8), or Dab2–2112 (lanes 3, 6, 9), as well as DAB2 and T7-Tag scramblase expression plasmids in ratios of 5:1:1 (lanes 1–3), 10:1:1 (lanes 4–6), and 25:1:1 (lanes 7–9), respectively. pCI-neo was used to bring up the total plasmid DNA to 7 μg. The total cell lysates were collected and subjected to Western blot analysis with p96 (DAB2), T7-Tag, and β-actin antibodies. D: Either pTOPO-U6 (upper panel) or Dab2–2112 (lower panel) was cotransfected with pEGFPC3-DAB2 and pDsRed1-N1 into K562 cells in a ratio of 5:1:1 for 48 h. Following transfection, the fluorescent intensity was observed by fluorescence microscopy.

cess (Fig. 2A). To unveil the consequences of DAB2 induction, several approaches were compared for the inhibition of DAB2 expression. First, FITC-labeled antisense S-oligos targeting the DAB2 translation initiation site were synthesized and transfected into K562 cells. Although more than 90% of the cells emitted a fluorescent signal that indicated good transfection efficiency (data not shown), the levels of TPA-induced DAB2 did not change (Fig. 2B, upper panel). Similarly, introducing DAB2 antisense PNA targeting both the 5′-untranslated region and the translation initiation site into K562 cells elicited no change of TPA-induced DAB2 expression (Fig. 2B, lower panel). To explore the use of DAB2 siRNA to modulate DAB2 induction, either Dab2–419 or Dab2–2112 was transfected into K562 cells followed by TPA treatment for 24 and 48 h (Fig. 2C). With a transfection efficiency of approximately 50%, Dab2–419 had a minimal effect in the suppression of DAB2 induction. In contrast, Dab2–2112 decreased the level of TPA-induced DAB2, consistent with its effect on the down-regulation of exogenous DAB2 expression (Fig. 1). These results suggest that DAB2–2112, but not the antisense S-oligos and PNA, is a powerful tool for modulating TPA-induced DAB2 gene expression.

3.3. *Dab2–2112 modulates cellular adhesive properties of K562 cells*

K562 cells grew in suspension culture as free-floating cells and formed cell aggregates within 24–48 h after TPA treatment (Fig. 3A). When observed under light microscopy after cytospin and Liu's stain, the TPA-treated cells exhibited typical megakaryocytic differentiation phenotypes with enlargement of the majority of cells, a decrease of the N/C ratio, and the presence of multiple lobes of nuclei (Fig. 3B). To delineate whether or not DAB2 induction associated with these phenotypic changes, we transfected Dab2–2112 into K562 cells followed by TPA treatment. We found that, in the Dab2–2112 expressing cells, the number of large cell aggregates (>5 cells/aggregate) decreased to approximately 46% of the vector-transfected control cells 48 h after TPA treatment. Concomitant with the decrease of cell aggregation, the adhesion and spreading of cells to tissue culture dishes increased for approximately 85% (Fig. 3A). In contrast, Dab2–2112 had no effect on the morphological changes and the up-regulation of integrin β3 associated with megakaryocytic differentiation (Fig. 3B). The effect of Dab2–2112 on K562 cell aggregations could not be analyzed in HEL and MEG-01 cells since both cell

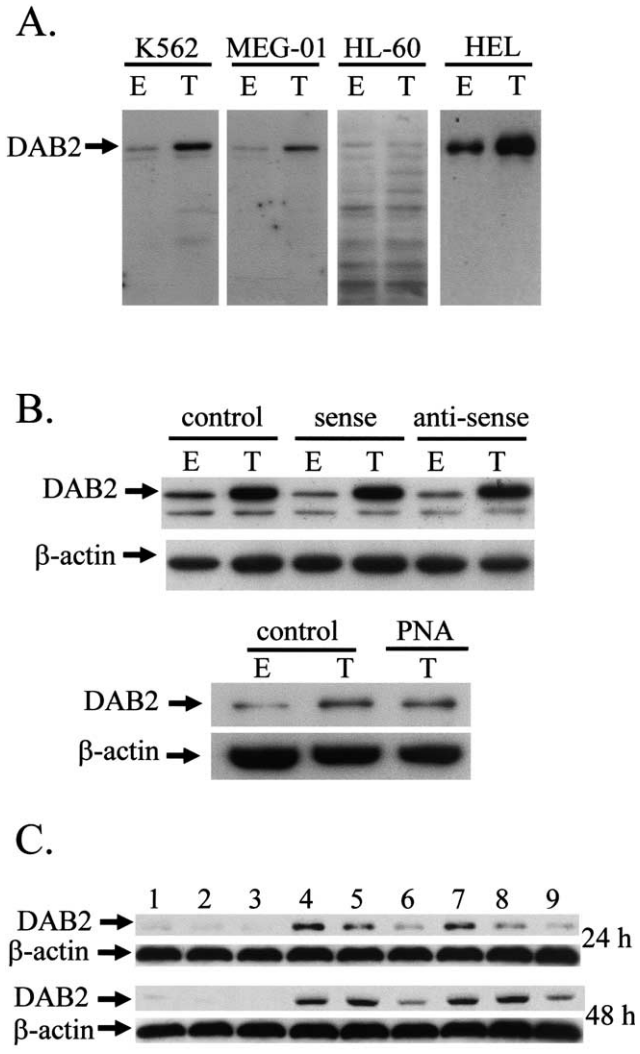

Fig. 2. Modulation of TPA-induced DAB2 expression by DAB2 antisense S-oligos, PNA, and siRNA. A: Expression of DAB2 in myeloid leukemic cell lines. K562, MEG-01, HL-60, and HEL cells were plated at a density of 1.5×10^4/ml. On the following day, cells were treated with TPA (10 ng/ml) or solvent control ethanol for 48 h. The cell lysates were collected and subjected to Western blot analysis with the p96 antibody. The increased background of the HL-60 cells was due to a longer exposure time of the film. B: Effects of antisense PNA and S-oligos on TPA-induced DAB2 expression. Non-transfected K562 cells (control) as well as K562 cells transfected with the DAB2 antisense PNA (lower panel), sense and antisense S-oligos (upper panel) were treated with TPA (T) or vehicle control ethanol (E) for 48 h. The cell lysates were collected for Western blot analysis with the p96 antibody and reprobed with β-actin for the control of equal loading. C: Effects of DAB2 siRNA on TPA-induced DAB2 expression. K562 cells were transfected with 6 μg pTOPO-U6 (lanes 1, 4, 7), Dab2–419 (lanes 2, 5, 8), and Dab2–2112 (lanes 3, 6, 9). At 24 h after transfection, the cell density was adjusted to 1.5×10^4/ml and the cells were subjected to treatment with 2 ng/ml (lanes 4–6) and 10 ng/ml (lanes 7–9) TPA, or solvent control ethanol (lanes 1–3). At 24 and 48 h after TPA treatment, cell lysates were collected for Western blot analysis with the p96 antibody. For control of equal loading, the membranes were reprobed with the anti-β-actin antibody.

types did not form cell clusters but attached to the tissue culture dish [15,16] shortly after TPA treatment (data not shown). These results suggest that DAB2 induction plays a role in the control of K562 cell–cell adhesion but is not involved in the megakaryocytic differentiation signals regarding morphological changes and β3 gene expression.

3.4. Dab2–2112 sustains p42/p44 MAPK phosphorylation/activation

Induction of DAB2 occurred in a time- and p42/p44 MAPK-dependent manner [9]. In this study, Western blot analysis with the anti-p96 antibody revealed maximum induction of DAB2 at 24–48 h after TPA treatment (Fig. 4A). Concurrently, the sustained activation of MAPK as detected by anti-phospho-p42/p44 MAPK antibody was drastically reduced. The temporal pattern of DAB2 expression and MAPK phosphorylation suggests a connection between DAB2 and MAPK in TPA signaling. This hypothesis was characterized further using the DAB2 siRNA. In this content, Dab2–2112 was transfected into K562 cells to suppress TPA-mediated DAB2 induction. Following TPA treatment for the indicated time, the phospho-specific p42/p44 MAPK antibody was used to analyze the level of MAPK activity. Of the cells expressing Dab2–2112, p42/p44 MAPK was still activated within 30 min after TPA treatment (data not shown). The data indicate that Dab2–2112 does not affect TPA-mediated p42/p44 MAPK activation. Instead, the Dab2–2112-transfected cells were found to have a higher level of p42/p44-MAPK phosphorylation (Fig. 4B). For instance, at 48 h after TPA treatment, Dab2–2112 reduced the magnitude of MAPK dephosphorylation and sustained MAPK activity to the level at 12–24 h of the control cells. These results suggest a role of DAB2 induction in the suppression of MAPK phosphorylation. To further evaluate this observation, we expressed pCI-neo-hDAB2 in K562 cells and analyzed the degree of MAPK phosphorylation. Consistent with the results of Dab2–2112, the phosphorylation of MAPK was diminished by DAB2 expression (Fig. 4C). Therefore, up-regulation of DAB2 plays a role in the decrease of MAPK activity after sustained TPA treatment.

4. Discussion

The lack of a simple genetic tool to inhibit DAB2 expression has complicated the investigation of DAB2 function in an in vitro cellular model, such as its up-regulation during megakaryocytic differentiation of K562 cells. Although antisense S-oligos and PNA have been used successfully in blocking gene expression of proteins such as GRB2, COX-2, and c-MYC [17–19], our attempts to down-regulate DAB2 by these approaches were ineffective. Transfection efficiency appears not to account for the failure because most of the transfected cells took up the oligonucleotides efficiently. That DAB2 antisense oligonucleotides proved ineffective is most probably due to targeting sequences that are not appropriate, given that there are few general rules to guide their design.

The recent development of the RNAi technique in mammalian cells has prompted us to explore the use of siRNA to moderate DAB2 expression. Of the DAB2 siRNAs tested, Dab2–419 is incapable of decreasing the levels of DAB2. The 1 bp mismatch in the dsRNA region of Dab2–419 may account for its loss in gene-specific silencing of DAB2. Alternatively, the targeting sequences of Dab2–419 may not be appropriate for the function of siRNA. Dab2–2112 is effective in the inhibition of DAB2 expression, regardless of the expression in wild type DAB2, EGFP-DAB2, or TPA-mediated

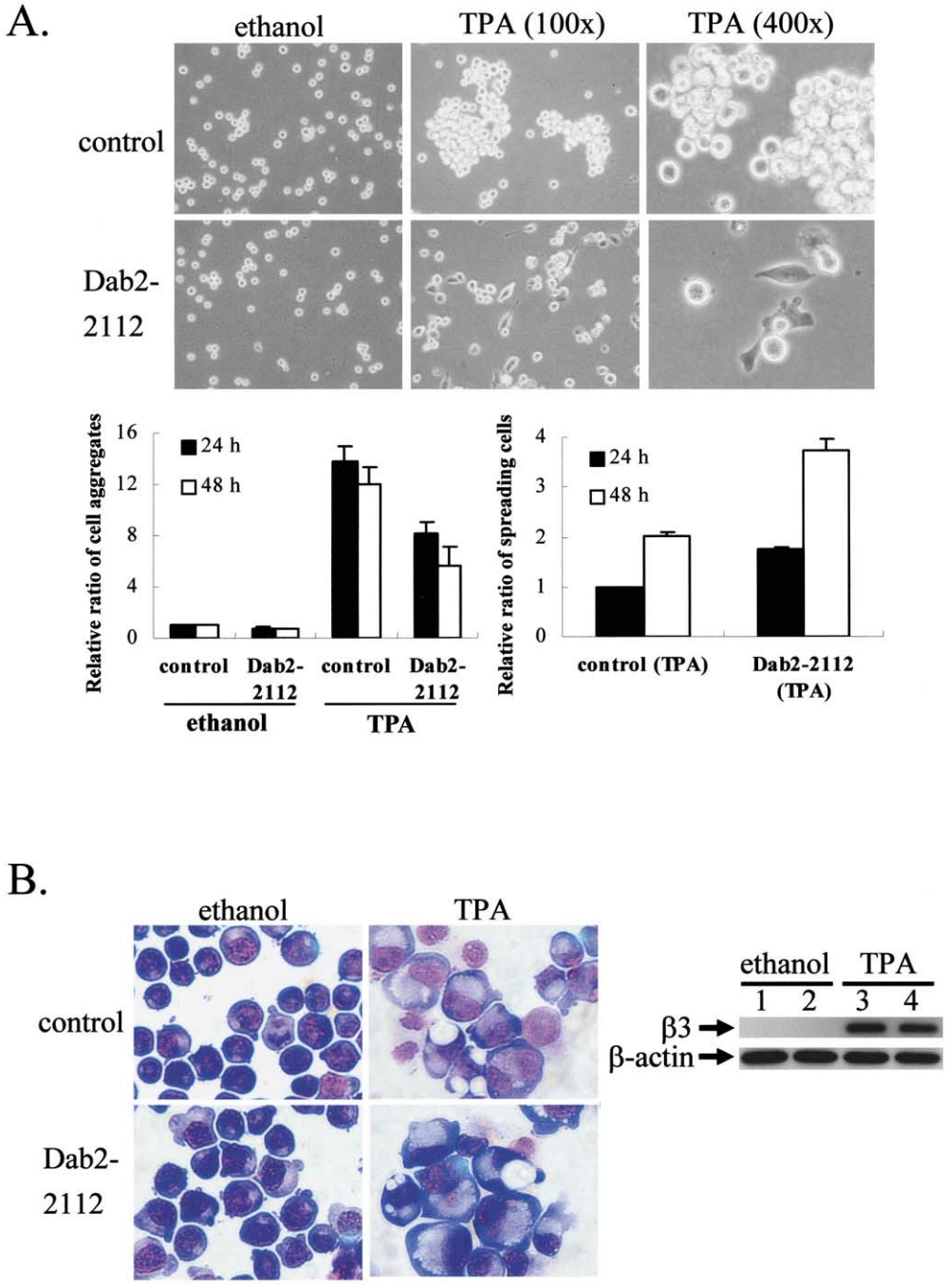

Fig. 3. Effects of Dab2–2112 on cellular adhesive function, morphological changes, and integrin β3 expression associated with megakaryocytic differentiation of K562 cells. A: Dab2–2112 dispersed TPA-induced cell aggregations. K562 cells were transfected with pTOPO-U6 (upper panel) and Dab2–2112 (lower panel) in the presence of LF2000 for 24 h. After adjusting the cell density to 3×10^4/ml, the cells were treated with ethanol or TPA for 48 h. The cell adhesive properties were observed with phase contrast microscopy and represented fields are shown (100×). Higher magnification fields (400×) for TPA-treated cells are also presented for the evaluation of the effect on spreading. The cell aggregates and cell spreading were quantified as described in Section 2 and are presented as the relative ratio to the control cells. In the cell aggregation assay, the numbers of cell aggregates in the 24 h ethanol-treated, pTOPO-U6-transfected control cells were arbitrarily set as 1. In the cell spreading assay, the numbers of spreading cells in the 24 h TPA-treated, pTOPO-U6-transfected control cells were arbitrarily set as 1. No spreading cells were observed in the ethanol-treated control cells. The data represented the average ± S.E.M. of two independent experiments with three assays in each experiment. B: Dab2–2112 had little effect on TPA-induced morphological changes and integrin β3 expression. Aliquots of cells from panel A were cytospun, stained with Liu's stain reagents, and observed by light microscopy. In addition, the lysates for K562 cells transfected with pTOPO-U6 (lanes 1 and 3) and Dab2–2112 (lanes 2 and 4) were subjected to Western blot analysis with anti-integrin β3 antibody. The expression of β-actin was used for the control of equal protein loading.

endogenous DAB2 induction. Most importantly, the inhibition is DAB2-specific. This notion is supported by the results showing that Dab2–2112 does not affect the expression of EGFP, RFP, and membrane protein scramblase. The specificity of Dab2–2112 has been further ensured by searches of the NCBI database. No sequence similarity was found between the Dab2–2112 targeting sequences and other known mRNA sequences. Therefore, these observations reveal that Dab2–

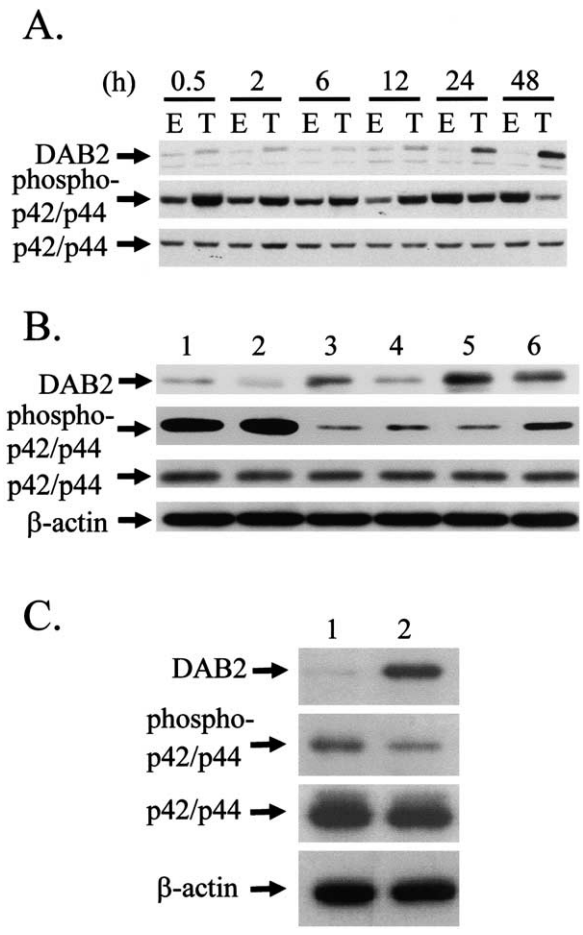

Fig. 4. Reciprocal regulation of DAB2 and MAPK in megakaryocytic differentiation of K562 cells. A: DAB2 expression and MAPK activation in TPA-treated K562 cells. K562 cells were plated at 1.5×10^4/ml and treated with 10 ng/ml TPA (T) or vehicle control ethanol (E) for the indicated time. The cell lysates were collected and analyzed by Western blot for the indicated proteins. B: DAB2 siRNA reduced the magnitude of MAPK dephosphorylation. K562 cells were transfected with 6 μg pTOPO-U6 (lanes 1, 3, 5) and Dab2–2112 (lanes 2, 4, 6) followed by treatment with TPA for 12 (lanes 1–2), 24 (lanes 3–4), and 48 (lanes 5–6) h. Cell lysates were collected for Western blot analysis of the indicated proteins. C: Expression of DAB2 down-regulated MAPK phosphorylation. K562 cells were transfected with vector control (lane 1) or pCI-neo-DAB2 (lane 2) for 48 h. Cell lysates were collected for Western blot analysis of the indicated proteins. The expression of β-actin was used for the control of equal protein loading.

2112 is a specific and functionally active modulator of DAB2 expression.

Megakaryocytic differentiation of K562 cells associates with changes in morphology, cellular adhesive properties, integrin β3 expression, and MAPK activation [20]. A recent study has revealed a role of DAB2 in the adhesion of RAW cells to laminin and collagen type IV [4]. This has prompted us to determine whether DAB2 plays any role in the cellular adhesive function of K562. The breakdown of cell aggregation by Dab2 siRNA suggests that, in addition to the regulation of cell–extracellular matrix adhesion [4], DAB2 is involved in the control of cell–cell adhesion when K562 cells undergo differentiation. The disruption of TPA-induced cell aggregates is DAB2-specific, since siRNAs targeting firefly luciferase and membrane protein scramblase do not affect the formation of cell aggregates (data not shown). We have noted that, although DAB2 induction also accompanies megakaryocytic differentiation of HEL and MEG-01 cells, these two cell types lack cell–cell adhesion and do not form cell aggregates in our assay condition. They adhere to the tissue culture dishes shortly after induction of differentiation. These observations suggest that induction of DAB2 is necessary but not sufficient to explain the cellular adhesive behavior of a particular cell type. An additional factor may be involved and act with DAB2 to control cell–cell adhesion. Alternatively, HEL and MEG-01 cells may require pathways other than K562 to produce adhesion. In support of this notion, these cell lines were shown to have distinct expression patterns for proteins involved in cell adhesion [21,22]. Furthermore, a differential inhibitory effect of α- and β-tocopherol on cell adhesion of K562 and HEL cells has been observed [23]. The detailed molecular mechanisms of DAB2 in regulating cell–cell adhesion are currently under investigation in our laboratory.

The present study also suggests that DAB2 may play a role in decreasing MAPK activity following sustained MAPK activation. This is consistent with reports that have demonstrated that DAB2 negatively regulates MAPK activity in several epithelial and macrophage cell lines [1,4]. Since we have shown that DAB2 is induced in a MAPK-dependent manner [9], our results further imply the presence of a reciprocal regulatory loop between DAB2 and MAPK. This regulation may represent a mechanism, in addition to protein kinase C down-regulation [24] and MAPK phosphatase activation [25], to control TPA and MAPK signaling and to maintain the cellular homeostasis status. In contrast to our results, a study using retinoic acid-induced F9 embryonic carcinoma cells shows that DAB2 does not affect MAPK activity and uncoupling of MAPK activation and *fos* suppression [26]. Therefore, the regulation between DAB2 and MAPK appears to be cell type-specific.

In summary, this study shows for the first time that a functional DAB2 siRNA is useful in the down-regulation of DAB2 expression. The results indicate a role of DAB2 in cell–cell adhesion and have revealed a mutual regulation between DAB2 and MAPK during K562 cell differentiation.

Acknowledgements: This work was supported in part by National Science Council Grant NSC-91-2314-B-182-036 and Chang Gung Memorial Hospital Grant CMRP1206 to C.P.T.

References

[1] Zhou, J. and Hsieh, J.T. (2001) J. Biol. Chem. 276, 27793–27798.
[2] Xu, X.X., Yang, W., Jackowski, S. and Rock, C.O. (1995) J. Biol. Chem. 270, 14184–14191.
[3] Hocevar, B.A., Smine, A., Xu, X.X. and Howe, P.H. (2001) EMBO J. 20, 2789–2801.
[4] Rosenbauer, F., Kallies, A., Scheller, M., Knobeloch, K.P., Rock, C.O., Schwieger, M., Stocking, C. and Horak, I. (2002) EMBO J. 21, 211–220.
[5] Wang, Z., Tseng, C.-P., Pong, R.C., Chen, H., McConnell, J.D., Navone, N. and Hsieh, J.T. (2002) J. Biol. Chem. 277, 12622–12631.
[6] Xu, X.X., Yi, T., Tang, B. and Lambeth, J.D. (1998) Oncogene 16, 1561–1569.
[7] Inoue, A., Sato, O., Homma, K. and Ikebe, M. (2002) Biochem. Biophys. Res. Commun. 292, 300–307.
[8] Tseng, C.-P., Ely, B.D., Pong, R.C., Wang, Z., Zhou, J. and Hsieh, J.T. (1999) J. Biol. Chem. 274, 31981–31986.
[9] Tseng, C.-P., Huang, C.H., Tseng, C.C., Lin, M.H., Hsieh, J.T. and Tseng, C.H. (2001) Biochem. Biophys. Res. Commun. 285, 129–135.

[10] Tseng, C.-P., Ely, B.D., Li, Y., Pong, R.C. and Hsieh, J.T. (1998) Endocrinology 139, 3542–3553.
[11] Mok, S.C., Chan, W.Y., Wong, K.K., Cheung, K.K., Lau, C.C., Ng, S.W., Baldini, A., Colitti, C.V., Rock, C.O. and Berkowits, R.A. (1998) Oncogene 16, 2381–2387.
[12] Fire, A., Xu, S., Montgomery, M.K., Kostas, S.A., Driver, S.E. and Mello, C.C. (1998) Nature 391, 806–811.
[13] Yu, J.Y., DeRuiter, S.L. and Turner, D.L. (2002) Proc. Natl. Acad. Sci. USA 99, 6047–6052.
[14] Tseng, C.-C. and Tseng, C.-P. (2000) FEBS Lett. 475, 232–236.
[15] Murate, T., Saga, S., Hamaguchi, M., Asano, H., Ito, T., Watanabe, T., Adachi, K., Koizumi, K.T., Yoshida, S. and Saito, H. (1995) Proc. Soc. Exp. Biol. Med. 209, 270–278.
[16] Papayannopoulou, T., Nakamoto, B., Yokochi, T., Chait, A. and Kannagi, R. (1983) Blood 62, 832–845.
[17] Tari, A.M., Hung, M.C., Li, K. and Lopez-Berestein, G. (1999) Oncogene 18, 1325–1332.
[18] Walker, T.L., Dass, C.R. and Burton, M.A. (2002) Anticancer Res. 22, 2237–2245.
[19] Nakanishi, Y., Kamijo, R., Takizawa, K., Hatori, M. and Nagumo, M. (2001) Eur. J. Cancer 37, 1570–1578.
[20] Alitalo, R. (1990) Leuk. Res. 14, 501–514.
[21] Hunakova, L., Sedlak, J., Klobusicka, M., Sulikova, M. and Chorvath, B. (1995) Neoplasma 42, 249–253.
[22] Ylanne, J., Cheresh, D.A. and Virtanen, I. (1990) Blood 76, 570–577.
[23] Breyer, I. and Azzu, A. (2001) Free Radic. Biol. Med. 30, 1381–1389.
[24] Hansen, L.A., Monteiro-Riviere, N.A. and Smart, R.C. (1990) Cancer Res. 50, 5740–5745.
[25] Bhalla, U.S., Ram, P.T. and Iyengar, R. (2002) Science 297, 1018–1023.
[26] He, J., Smith, E.R. and Xu, X.X. (2001) J. Biol. Chem. 276, 26814–26818.